 DOI 10.1109/IGARSS52108.2023.10281464

UPDATED IONOSPHERIC MODULE FOR ESA BIOMASS MISSION END-TO-END PERFORMANCE SIMULATOR

A. Camps[1,2], *J. Barbosa*[3], *I. Nestoras*[3], *A. Jordão*[3], *M. J. Sanjuan-Ferrer*[4], *M. Rodriguez-Cassola*[4], *V. Queiroz de Almeida*[4], *F. Betancourt-Payan*[4]

[1]CommSensLab-UPC– Dep. of Signal Theory and Communications, and IEEC/CTE-UPC, Universitat Politècnica de Catalunya - Campus Nord, E-08034 Barcelona, SP
[2]ASPIRE Visiting International Professor, UAE University, CoE, PO Box 15551, Al Ain, UAE.
[3]RDA - Research and Development in Aerospace GmbH, Zürich, CH
[4]German Aerospace Center (DLR), Microwaves and Radar Institute, Oberpfaffenhofen, 82234 Weßling, DE
E-mail: adriano.jose.camps@ upc.edu

ABSTRACT

ESA's BIOMASS is the seventh Earth Explorer mission. It will be devoted to the global monitoring of: 1) above ground forest biomass and biomass change maps with an accuracy < 20%, a 100-200 m spatial resolution, and 6-12 months temporal resolution; 2) global forest disturbance maps with a classification accuracy > 90%, a 50-200 m spatial resolution, and 2-12 months temporal resolution; and 3) global forest height maps with an accuracy of 20-30%, 100 m spatial resolution, and 12 months temporal resolution.

BIOMASS is based on a P-band SAR (438 MHz center frequency, 6 MHz bandwidth) orbiting in a dawn-dusk, Sun-synchronous orbit at 674 km, that will systematically acquire fully- (quad-) polarized image data in an interferometric mode over all major forested areas on the globe and a tomographic phase (7 images) to retrieve forest vertical structure information. At P-band ionospheric effects are very important and need to be corrected for. This paper describes the current status of the Ionospheric module for the Biomass End-to-end Performance Simulator (BEEPS-IOM).

Index Terms— Ionosphere, scintillation, intensity, phase, Faraday rotation, dispersion.

1. INTRODUCTION

ESA's BIOMASS is the seventh Earth Explorer mission [1]. Over the past 3 years UPC/IEEC and RDA have been developing for DLR the Ionospheric module for the BIOMASS End-to-End Performance Simulator (BEEPS). Preliminary progress results were presented in IGARSS 2021 [2]. In IGARSS 2023 the final version of the simulator will be presented. Figure 1 shows the block diagram of the module that simulates the ionospheric effects on propagation of electromagnetic waves, including:

- low-frequency effects (group delay, phase advance, dispersion, losses and Faraday rotation angle,) [3] are associated to slowly varying electron density profiles, and the associated Total Electron Content (TEC), as derived from the combination of IRI/NeQuick VTEC modelling, the stochastic (slow) TEC variability not captured by climatological models and the equatorial plasma bubbles (EPB) with their Eastward drift.
- high-frequency effects (intensity and phase scintillations) are formulated using Rino's Multiple Phase Screen model [4] with several configurable inputs, including a variable screen height (as given by the maximum of the electron density profile in each point), and a horizontal drift of the ionosphere. Several of the high frequency inputs can be obtained directly from the WBMOD model outputs[1] if selected by the user

It is worth noting that random and moving electron density inhomogeneities not only introduce rapid intensity (i.e. "losses") and phase fluctuations, but also high-frequency fluctuations of the ionospheric delay, and Faraday rotation angle.

Currently, all the BEEPS-IOM interfaces to compute the TEC from the electron density profiles provided by IRI or NeQuick and to use the IGRF model, gAGE stochastic TEC, and EPB models have been completed and validated, as well as the interfaces to read IONEX files, and the implementation of the mapping function. Signal disturbances (delay, phase, losses, Faraday rotation, and fast scintillations) have also been completed and validated.

2. LOW-FREQUENCY EFFECTS

The calculation of the ionospheric effects requires first to compute the Slant Total Electron Content (STEC) from the

[1] WBMOD is not part of this software package, and its outputs are obtained independently and used as inputs of this simulator.

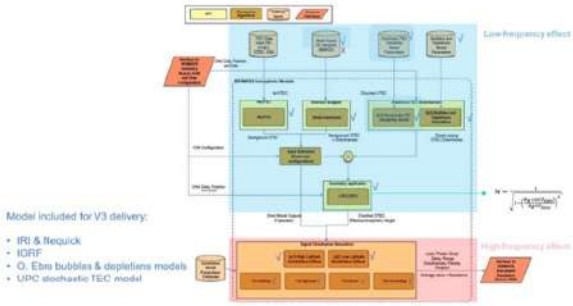

Fig. 1. IOM-BEEPS software architecture indicating low- and high-frequency ionospheric effects, models, and their inputs.

Vertical Total Electron Content (VTEC), using the mapping function (see Fig. 1), and including the TEC Stochastic variability as well as bubbles and depletions contributions. The VTEC is estimated from the numerical integration of the electron density, from either IRI [6] or NeQuick [7], over a vertical column at a particular location and time.

Figures 2 and 3 show sample VTEC and magnetic field simulated for one full orbit of BIOMASS. The magnetic field is calculated according to the IGRF model at the Ionospheric Piercing Points (IPP) onto a layer placed at the height of maximum ionization (ionospheric height).

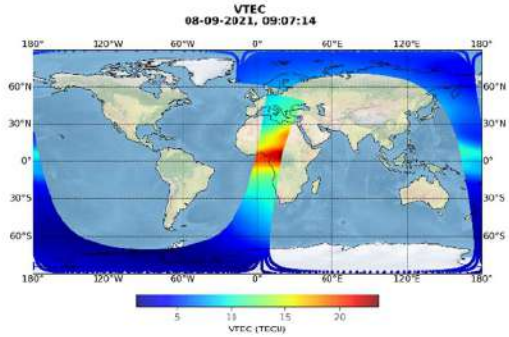

Fig. 2. IOM-BEEPS simulated Vertical Total Electron Content (VTEC).

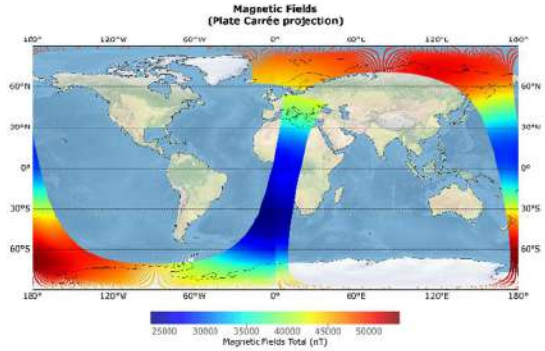

Fig. 3. IOM-BEEPS simulated Earth's magnetic field at a height of 350km.

2.1. Delay, Phase and Dispersion

The envelope of the signal suffers a positive delay (in meters or in seconds) as given by:

$$\Delta^{iono}_{gr,f\ [m]} = +\frac{40.3 \cdot 10^{16}}{f^2_{[Hz]}} \cdot STEC(t)_{[TECU]} \quad (1a)$$

$$\Delta^{iono}_{gr,f\ [s]} = +\frac{1.345 \cdot 10^{-7}}{f^2_{[Hz]}} \cdot STEC(t)_{[TECU]} \quad (1b)$$

The phase measurements suffer advancement when crossing the ionosphere given by:

$$\Delta^{iono}_{ph,f\ [m]} = -\frac{40.3 \cdot 10^{16}}{f^2_{[Hz]}} \cdot STEC(t)_{[TECU]} \quad (2)$$

This phase advancement can be converted into wavelengths by dividing by the electromagnetic wavelength ($\lambda = c/f$), and into radians by subsequent multiplication by 2π.

From the Eqn. (1) a simplified expression for the signal dispersion due to the finite bandwidth can be estimated as:

$$D^{iono}_{[s/Hz]} = \frac{\partial \Delta^{iono}_{gr,f\ [s]}}{\partial f_{[Hz]}} = -\frac{2.690 \cdot 10^{-7}}{f^3_{[Hz]}} \cdot STEC(t)_{[TECU]} \quad (3)$$

Figures 4, 5, and 6 show sample delay, phase, and dispersion simulated for a full orbit of BIOMASS.

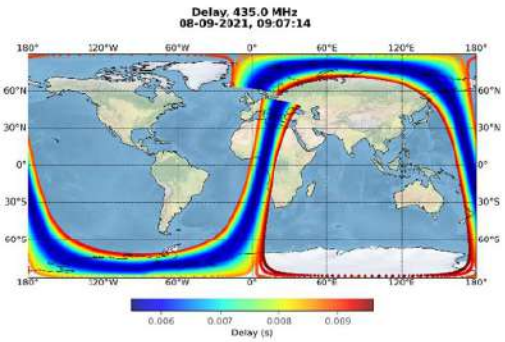

Fig. 4. IOM-BEEPS simulated ionospheric delay.

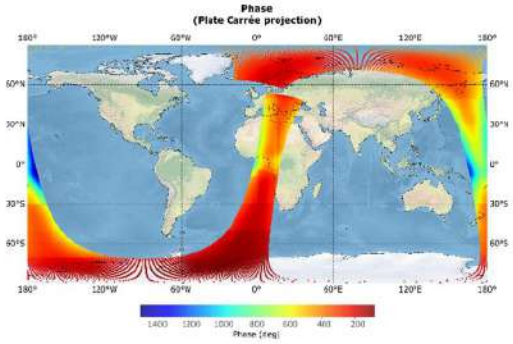

Fig. 5. IOM-BEEPS simulated phase advance.

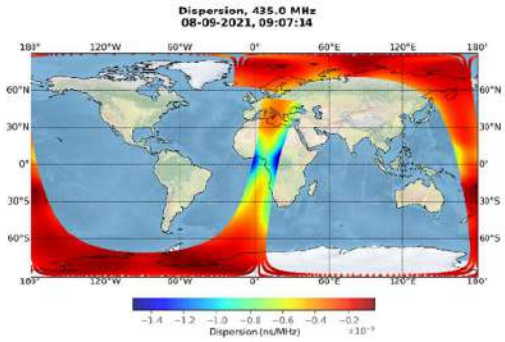

Fig. 6. IOM-BEEPS simulated dispersion.

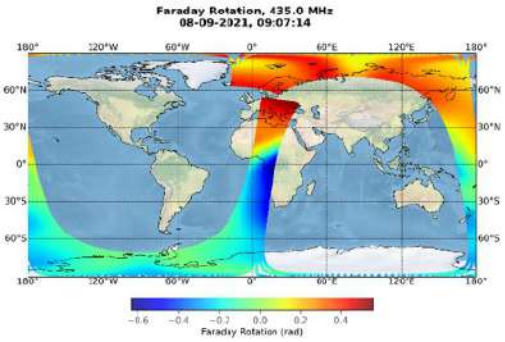

Fig. 8. IOM-BEEPS simulated Faraday rotation

2.2. Losses and Faraday rotation:

Ionospheric losses above VHF are very small, but increase at lower frequencies. In fact, for an example frequency of 435MHz, the one-way absorption (in [dB]) has an average value of ~0.010 dB at mid-latitudes for a zenith path. At polar and auroral regions the average absorption is ~0.045 dB for zenith path [9]. From 45° to 65° latitude a linear transition is assumed. As compared to all other propagation losses and intensity scintillation, this effect is negligible. Figure 7 shows a sample ionospheric absorption simulated for a full orbit of BIOMASS.

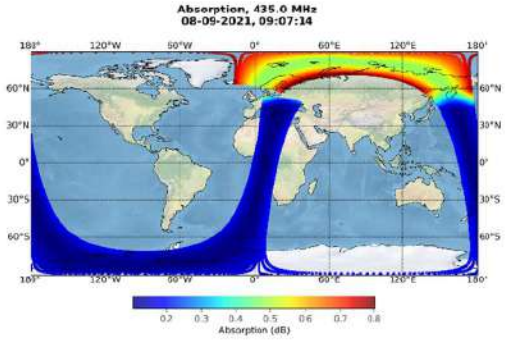

Fig. 7. IOM-BEEPS simulated absorption.

The calculation of the Faraday rotation requires the evaluation of the magnetic field of the Earth, using e.g. the IGRF-13 model [5], which provides the North-East-Up components ($\vec{B}_{NEU}$). The angle between the magnetic field ($\vec{B}_{xyz}$ in ECEF coordinates), and the wave propagation direction ($\vec{k}$) is computed by means of the scalar product of the normalized vectors:

$$cos(\theta) = \hat{k} \cdot \hat{B}_{xyz}. \quad (4)$$

Finally, the Faraday rotation can be computed as:

$$\varphi_{Faraday} = \frac{1.352 \cdot 10^{11}}{f^2_{[Hz]}} STEC(t)_{[TECU]} \left\| \vec{B}_{NEU} \right\| cos(\theta), \quad (5)$$

where the electric field polarization vector rotates clockwise if $\varphi > 0$º. Figure 8 shows a sample Faraday rotation simulated for a full orbit of BIOMASS.

3. HIGH-FREQUENCY EFFECTS

High-frequency effects (intensity and phase scintillations) are formulated using Rino's Multiple Phase Screen model [4]. However, in [4], the geophysical parameters, such as the TEC, the magnetic field, the ionospheric height at which the peak of the electron density is (and so is Rinos' phase screen). are assumed to be constant, which in real life they are not, as they vary along the orbital position. A particularity of UPC/IEEEC and RDA implementation of Rino's model, lies in the fact that the long strip can be divided into smaller tiles, allowing for the geophysical parameters to vary per tile. The tiles are designed to be large enough to accommodate (i.e. fit) the largest scales of the ionospheric irregularities, but small enough so that the Earth's magnetic field and VTEC variability inside them are negligible.

The assumption that the Earth's magnetic field and geometry do not change significantly within a "tile" (i.e. Rino's model output) has also been assessed for two different cases at equatorial and polar latitudes (see Fig. 9), finding a maximum phase difference of ~ 0.015 rad (~ 0.85°), and a maximum intensity difference of ~ 0.1 dB. These differences are small enough so that results can be considered qualitatively the same.

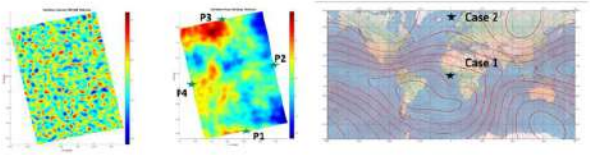

Fig. 9. Sample snap-shot ("tile") of the IOM-BEEPS high-frequency ionospheric effects: (left) intensity scintillation (±0.6 $dB_{peak\text{-}to\text{-}peak}$), (center) phase scintillation models (-40°, +60°), and (right) case studies #1 (5.15°, -3.77°) and #2 (60.54°, -7.58°) used to assess the goodness of the approximation that the Earth's magnetic field and geometry do not change significantly within a "tile" (point P1, P2, P3 and P4, wrt. to central point of the "tile").

Finally, Figs. 10 and 11 show the intensity and phase scintillations, respectively. These images are "frozen" as they correspond to the time the S/C is transiting and looking to the

side. Despite this the images have also a horizontal translation at moderate speeds, that are inferred from the WBMOD [8,9].

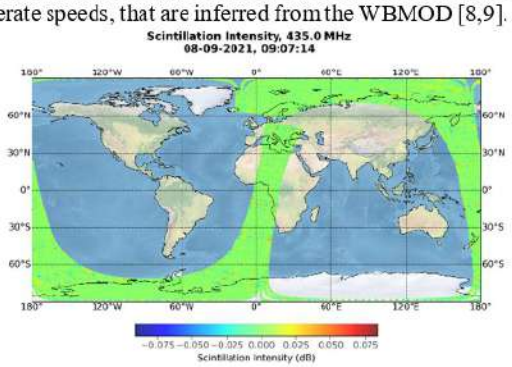

Fig. 10. IOM-BEEPS simulated ionospheric intensity scintillation.

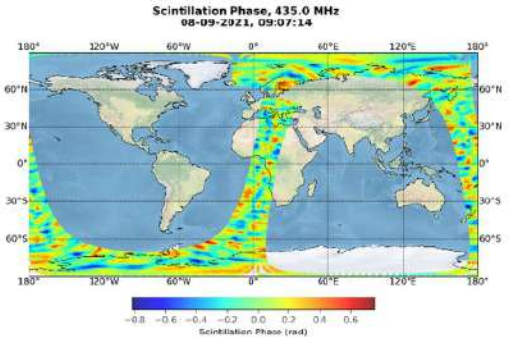

Fig. 11. IOM-BEEPS simulated ionospheric phase scintillation.

3. CONCLUSIONS

The BEEPS-IOM tool is a powerful tool that is currently being used by DLR to infer the effects of the ionosphere in ESA BIOMASS observables, and to derive mitigation algorithms, notably focusing algorithms, and to compensate for the signal dispersion. It is planned that during the mission operations, the simulator will ingest estimations of the actual ionospheric parameters at the time the S/C is passing.

4. REFERENCES

[1] ESA BIOMASS Mission: https://directory.eoportal.org/web/eoportal/satellite-missions/b/biomass (last visited May 2023)

[2] A. Camps, J. Barbosa, I. Nestoras, A. Jordão, M. J. Sanjuan-Ferrer and M. Rodriguez-Cassola, "Biomass End-to-End PErformance Simulator: Description of the Ionosphere Module," 2021 IEEE International Geoscience and Remote Sensing Symposium IGARSS, 2021, pp. 2266-2269, doi: 10.1109/IGARSS47720.2021.9554570.

[3] Recommendation ITU-R P.531-14: "Ionospheric propagation data and prediction methods required for the design of satellite networks and systems," available online at: https://www.itu.int/rec/R-REC-P.531-14-201908-I/en (last visited January 2023)

[4] C. Rino, "The Theory of Scintillation with Applications in Remote Sensing," ed. Wiley-IEEE Press, 2011 [Chapter 4 and Appendix 2].

[5] International Geomagnetic Reference Field: the 13th generation, Alken, P., Thébault, E., Beggan, C.D. et al. International Geomagnetic Reference Field: the thirteenth generation. Earth Planets Space 73, 49 (2021).doi: 10.1186/s40623-020-01288-x

[6] D. Bilitza, Pezzopane, M., Truhlik, V., Altadill, D., Reinisch, B. W., & Pignalberi, A. (2022). The International Reference Ionosphere model: A review and description of an ionospheric benchmark. Reviews of Geophysics, 60, e2022RG000792. https://doi.org/10.1029/2022RG000792

[7] G. Giovanni, and S.M. Radicella, 1990. An analytical model of the electron density pro_le in the ionosphere. Advances in Space Research. 10(11), pp. 27-30.

[8] J.A. Secan, R.M. Bussey E.J. Fremouw S. Basu, An improved model of equatorial scintillation. Radio Science. 1995;30(3):607-617. DOI: 10.1029/94RS03172

[9] J.A. Secan R.M. Bussey E.J. Fremouw S. Basu S. High-latitude upgrade to the wideband ionospheric scintillation model. Radio Science. 1997;32(4):1567-1574. DOI: 10.1029/97RS00453